

# Quality Factor Enhancement of Optical Channel Drop Filters Based on Photonic Crystal Ring Resonators

Aghil Shaverdi, Mohammad Soroosh\*, and Ehsan Namjoo

Department of Electrical Engineering, Shahid Chamran University of Ahvaz, Ahvaz, Iran

\*Corresponding Author's Email: m.soroosh@scu.ac.ir

Received: Aug. 6, 2017, Revised: Sep. 5, 2017, Accepted: Sep. 20, 2017, Available Online: Dec. 1, 2018

DOI: 10.29252/ijop.12.2.129

**ABSTRACT**— In this paper, a channel drop ring resonator filter based on two dimensional photonic crystal is proposed which is suitable for all optical communication systems. The multilayer of silicon rods in the center of resonant ring enables one to adjust resonant wavelength of the ring and enhance power coupling efficiency between ring and waveguide. Refractive index and radius of multilayer rods inside the ring are important factors which help one to enhance the desired output parameters. The proposed structure is capable of presenting high quality factor near 1937 in conjunction with 0.8 nm pass band. The high coupling efficiency 99% is another advantage of the proposed filter.

**KEYWORDS:** Optical filter, Photonic bandgap, Photonic crystal, Quality Factor.

## I. INTRODUCTION

The increasing demand of high-performance systems for metropolitan and access optical communications has led the development of devices and techniques which can employ the high capacity of optical communication in the best manner. Dense Wavelength Division Multiplexing (DWDM) is an effective technique which can use the optimum capacity of a single optical fiber [1] and [2].

Photonic Crystals (PCs) are periodic structures which can control behavior of light. PCs can cause stop bands, namely photonic band gaps (PBGs), for electromagnetic waves (EMs), in which the propagation of optical waves is forbidden [3]. If the periodicity of PCs be broken by some defects, the localization of EM field would be around the defect volume

[4]. By creating the defect layer or defect point in the PCs and subsequently breaking their periodicity, a defect mode can be produced inside the PBG. This defect mode leads to a high transmittance in the frequency (or wavelength) domain which can be used for designing a narrow band transmission spectra and high quality factor in a small area. These features made PCs as good candidates in optical communication such as optical filters [5],[6], demultiplexers [7],[13].

Optical channel drop filters (OCDFs) are essential components of photonic integrated circuits (PICs) and DWDM optical communication systems [8]. The first report on photonic crystal ring resonators (PCRRs) was in a hexagonal waveguide ring laser cavity [9]. Since then, significant progress has been made on CDFs in the areas of high spectral selectivity, spectral tunability, quality factor (QF), and pass band ( $\Delta\lambda$ ). The QF is  $\lambda/\Delta\lambda$  where  $\lambda$  is wavelength. The passband is the frequency (or wavelength) range of the filter that allows light to pass. In this case, the light power at output port respect to input port is more than 0.5. The quality factor of single ring resonator filters has been enhanced from 160 to over 1000 [10]-[14]. Rakhshani *et al.* proposed a PC-based filter using ring resonator with a QF of 842 [11]. Robinson *et al.* reported a two dimensional PC ring resonator based add-drop filter (ADF) with 13 nm of bandwidth and 114.69 of quality factor [13]. Mehdizadeh *et al.* proposed a structure in which  $\Delta\lambda$  and QF values were 4.5 nm and 344 respectively [14].

In this paper, based on completely circular PCRRs, we propose an OCDF which is able to drop different wavelengths. In this structure, average power transmission efficiency ( $P_{CE}$ ) is approximately 99% in conjunction with 0.8nm for pass band, and quality factor as high as 1937.  $P_{CE}$  is the ratio of light power at output port to input light power. These characteristics are highly suitable for full-ring based filters. The overall size of the proposed structure is  $432 \mu\text{m}^2$  which makes it appropriate for PICs. The paper is further organized as following: in section 2, we will present the proposed structure. In section 3, the results are discussed and finally the conclusion will be provided.

## II. THE PROPOSED STRUCTURE

The proposed structure consists of 31 and 21 circular rods in x and z directions respectively. The lattice constant (a) and the radius of basic rods are equal to 797nm and 190nm respectively. The refractive indices of background and silicon rods are 1 and 3.47 respectively. We use Plane Wave Expansion (PWE) method to calculate band structure of the proposed structure. Four PBGs at TM polarization were obtained and displayed in dark area in Fig. 1. It can be seen that the second PBG is in the range of  $0.46 < a/\lambda < 0.53$  (or  $1495 < \lambda < 1732$  nm) and is suitable for optical communication applications.

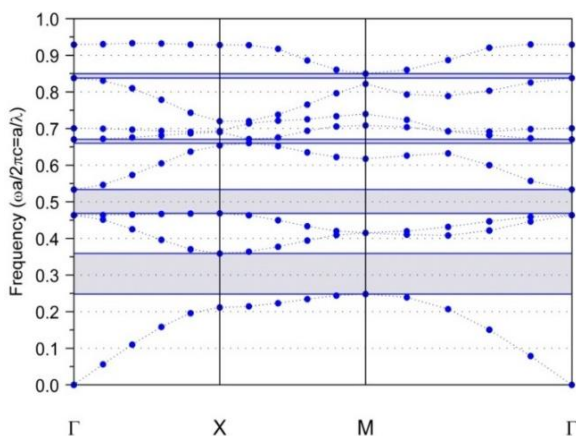


Fig. 1. Bandgap diagram of the proposed structure.

### A. Filter Design

To manipulate the light, two rows as waveguides and a circle as resonant ring between them are removed as shown in Fig. 2-

a. To create the resonator ring, we removed a  $5 \times 5$  square of rods and then placed a circular multilayer structure included green, blue and yellow rings in center of resulting empty area (Fig. 2-b). The red rods are the basic rods and 12 green rods make the exterior layer which are denoted by  $R_g$  as their radii and  $n$  as their refractive indices. 12 blue rods and 6 yellow rods with same refractive indices,  $n_b$  and  $n_y$ , form the interior layers which are marked by  $R_b$  and  $R_y$  as their radii respectively.

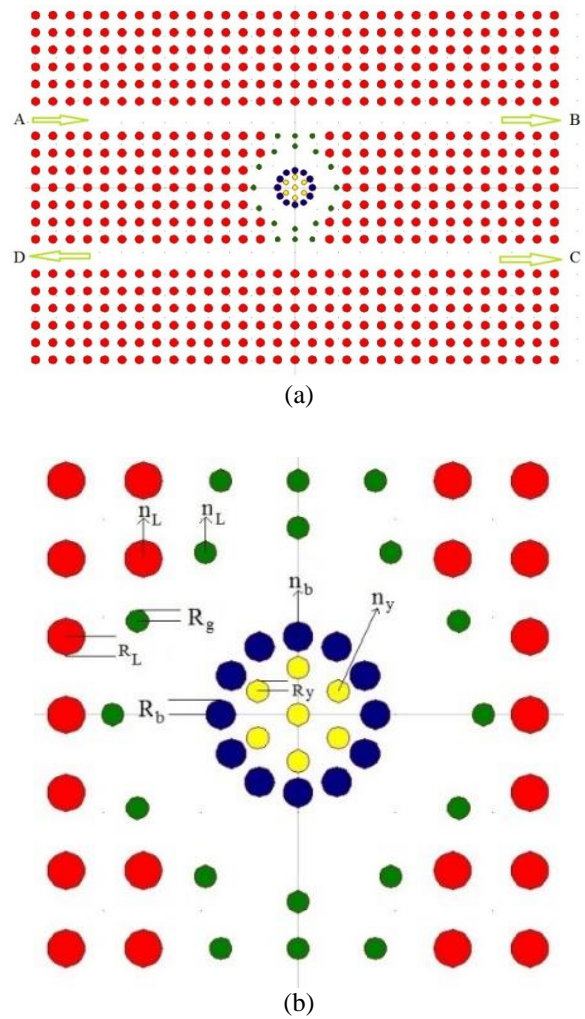


Fig. 2. (a) The schematic diagram of the proposed filter, (b) a macroscopic view of the resonant ring.

In the upper waveguide, the light power is launched at port A and is propagated to port B. If the wavelength of the light is equal to resonant wavelength of the ring, light can drop to the lower waveguide and propagate to ports C and D which are known as forward and

backward dropping respectively. To achieve the appropriate coupling between the waveguides and ring resonators, we matched the rods of the ring resonator with waveguides, where the coupling was exactly happening. By changing the radius of inner rods inside the resonator, the resonant frequency of resonator could be changed. Besides, we chose the refractive indices of the rods which are centered in the ring resonator lower than the major resonator so it could act as a reflector and the light could be confined and be propagated more and more near the surface. By using multilayer rings, light can be confined closer to the surface of the ring. The result of the greater confinement of light near the surface is a higher quality factor [15].

The refractive index and radius of rods in ring resonator are given in Table 1. Generally, we use the letters n and R as refractive index and radius of rods and employ indices L, g, b, and y for lattice (or basic), green, blue and yellow rods respectively.

Table 1. The value of parameters for resonant ring.

| Rod              | Green | Blue | Yellow |
|------------------|-------|------|--------|
| Refractive index | 3.58  | 3.4  | 3.4    |
| Radius (nm)      | 114   | 153  | 163    |

## B. Results and Discussion

In this work, we used RSoft software which employed the finite difference time domain (FDTD) method to simulate the behavior of light waves in the filter. The Gaussian input signal was launched in port A. The output spectrums at ports B, C and D are shown in Fig. 3.

Fig. 3 demonstrates the wavelength 1550nm can be dropped from upper into lower waveguides and propagated toward port C. This means that the proposed ring resonator has been tuned at 1550 nm. One can see  $P_{CE}$  at this wavelength is approximately 99% and  $\Delta\lambda$  is 0.8 nm. Consequently, QF is obtained 1937 that is suitable in comparison with other works based on PCRR [16]-[22] as given in Table 2.

Figure 4a demonstrates the ring resonator drops incoming light at wavelength 1550nm to

the lower waveguide, while it don't at wavelength 1560nm (Fig. 4b). As the both wavelengths are located in the PBG region, they can't scatter in the structure and propagate in the waveguides.

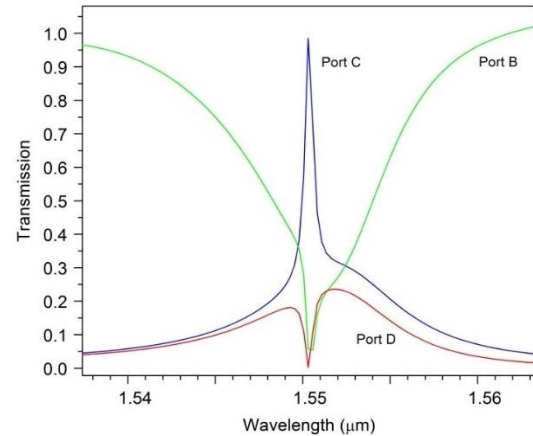


Fig. 3. Output spectra at B, C and D ports.

Table 2. Obtained results compared to other works.

| Reference | QF   | $P_{CE}$ (%) | $\Delta\lambda$ (nm) |
|-----------|------|--------------|----------------------|
| [16]      | 153  | 98           | 9.8                  |
| [17]      | 423  | 97           | 3.698                |
| [18]      | 840  | 100          | 1.845                |
| [19]      | 775  | 100          | 2                    |
| [20]      | 196  | 100          | 7.9                  |
| [21]      | 221  | 100          | 7                    |
| [22]      | 1330 | 95           | 1.16                 |
| [23]      | 98   | 100          | 19                   |
| [24]      | 283  | 96.4         | 5.48                 |
| This work | 1937 | 99           | 0.8                  |

If  $R_L$ , the radius of green rods, is changed from 189nm to 193nm, the central wavelength ( $\lambda_{ct}$ ) at port C will obtain from 1541nm to 1558nm (Fig. 5). One can conclude as  $R_L$  is increasing, the central wavelength at port C becomes longer while pass band and power coupling efficiency are almost constant (Table 3). Besides, the greater  $R_L$  results in the higher quality factor.

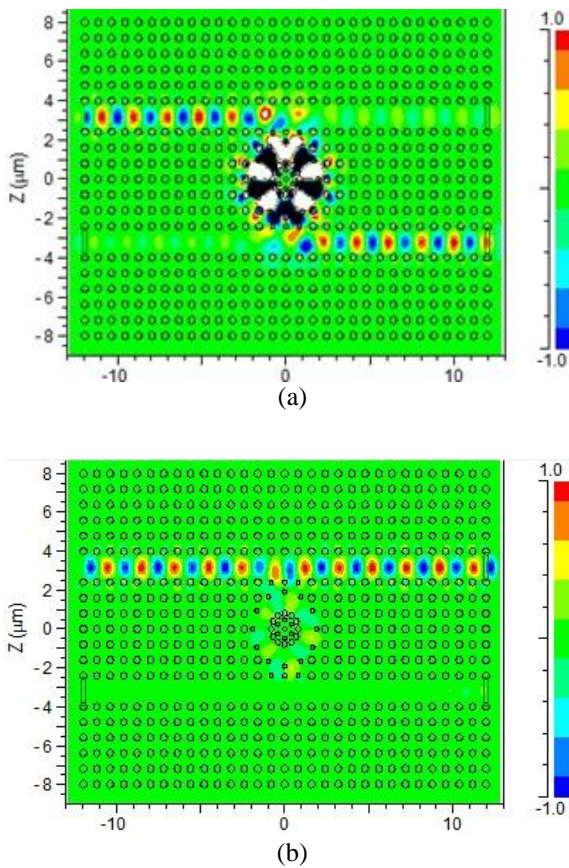


Fig. 4. The calculated electric field distribution inside the structure at two wavelengths (a) 1550 nm, and (b) 1560 nm.

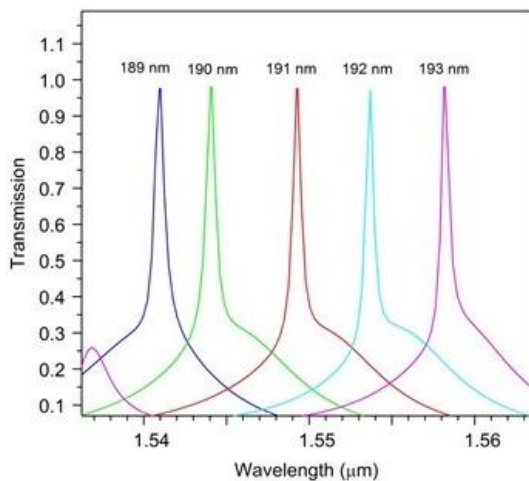


Fig. 5. The output spectrum at port C with different values of  $R_L$ .

Figure 6 demonstrates that changing the radius of blue rods ( $R_b$ ) from 151nm to 155nm shifts  $\lambda_{ct}$  to the upper wavelengths. Although one can obtain 0.5nm for pass band,  $P_{CE}$  is reduced to 70% with  $R_b=155$ nm. Table 4 shows the details of the output spectrum for different values of  $R_b$ .

Table 3. The output characteristics of the filter versus values of  $R_L$ .

| $R_L$ (nm) | $\Delta\lambda$ (nm) | $\lambda_{ct}$ (nm) | QF   | $P_{CE}$ (%) |
|------------|----------------------|---------------------|------|--------------|
| 189        | 1                    | 1541                | 1541 | 99           |
| 190        | 1                    | 1544                | 1544 | 100          |
| 191        | 1                    | 1549                | 1549 | 100          |
| 192        | 1                    | 1554                | 1554 | 97           |
| 193        | 1                    | 1558                | 1558 | 100          |

Simulation results show that the central wavelength at port C shifts to higher wavelengths when the radius of yellow rods ( $R_y$ ) is increasing (Fig. 7). According to Table 5, one could enhance  $P_{CE}$  to 98% and reduce pass band to 0.7nm if 112nm is selected to  $R_y$ . The effective refractive index is a key parameter and depends on refractive index and radii of rods. These wavelength shifts are due to change in the effective refractive index. By increasing the radius of rods, the effective refractive index increases so the wavelength shifts toward upper values.

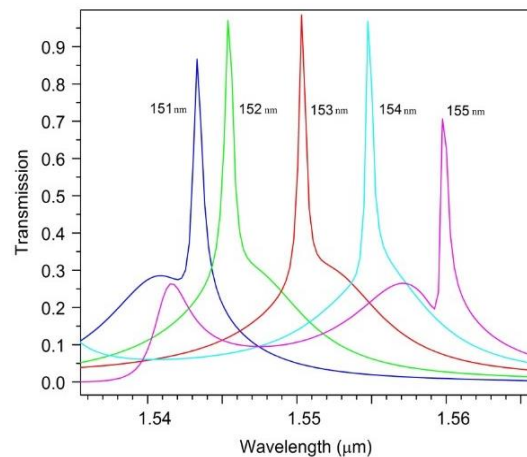


Fig. 6. The output spectrum with different values of  $R_b$ .

Table 4. The important parameters of the device with different values of  $R_b$ .

| $R_b$ (nm) | $\Delta\lambda$ (nm) | $\lambda_{ct}$ (nm) | QF   | $P_{CE}$ (%) |
|------------|----------------------|---------------------|------|--------------|
| 151        | 0.8                  | 1543                | 1928 | 86           |
| 152        | 0.95                 | 1545                | 1626 | 97           |
| 153        | 0.8                  | 1550                | 1937 | 99           |
| 154        | 0.7                  | 1555                | 2214 | 97           |
| 155        | 0.5                  | 1560                | 3120 | 70           |



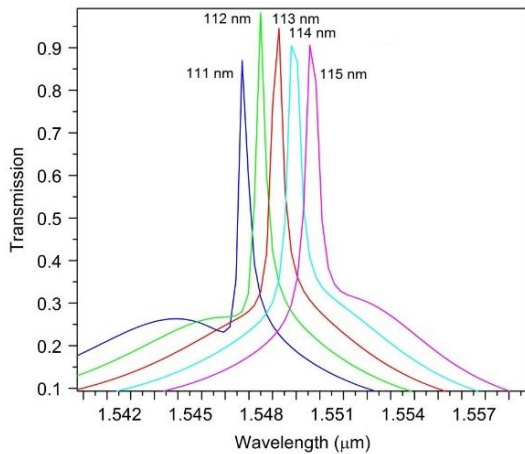


Fig. 7 The output spectrum of the filter for different values of  $R_y$ .

As shown in Fig. 8, the more refractive index of the basic rods results in higher central wavelengths at port C while pass band is almost equal to 1nm. One can see in Table 6,  $P_{CE}$  is approximately 99% if the refractive index of the basic rods to be 3.5.

Table 5. The output parameters of the filter as a function of  $R_y$ .

| $R_y$ (nm) | $\Delta\lambda$ (nm) | $\lambda_{ct}$ (nm) | QF   | $P_{CE}$ (%) |
|------------|----------------------|---------------------|------|--------------|
| 111        | 0.7                  | 1547                | 2210 | 87           |
| 112        | 0.7                  | 1548                | 2211 | 98           |
| 113        | 0.8                  | 1549                | 1936 | 94.5         |
| 114        | 0.75                 | 1550                | 2066 | 90.5         |
| 115        | 0.8                  | 1551                | 1938 | 90.5         |

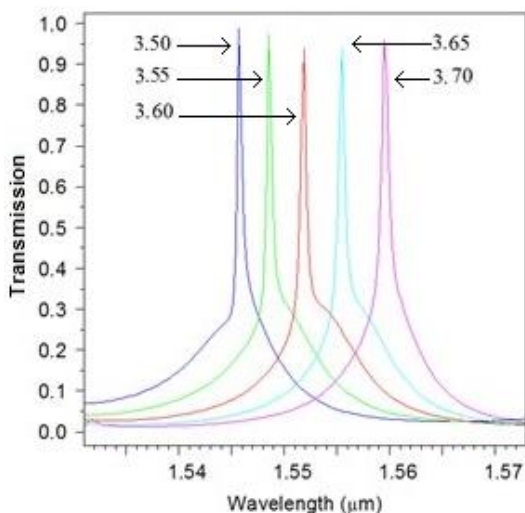


Fig. 8 The light power at port C with different values of  $n_L$ .

Figure 9 reveals the refractive index of blue and yellow rods is as an effective factor on central wavelength and power coupling

efficiency. This figure proves higher central wavelengths are obtained if refractive index of the mentioned rods is raised. As it's shown in Table 7, exact light transmission is occurred from port A to port C when refractive indices of alluded rods are equal to 3.36. In this case, pass band is obtained 1nm.

Table 6. The calculated output parameters of the filter for different values of  $n_L$ .

| $n_L$ | $\Delta\lambda$ (nm) | $\lambda_{ct}$ (nm) | QF   | $P_{CE}$ (%) |
|-------|----------------------|---------------------|------|--------------|
| 3.50  | 1                    | 1546                | 1546 | 99           |
| 3.55  | 1                    | 1548                | 1548 | 98           |
| 3.60  | 1                    | 1552                | 1552 | 96           |
| 3.65  | 1                    | 1555                | 1555 | 96           |
| 3.70  | 1                    | 1559                | 1559 | 98           |

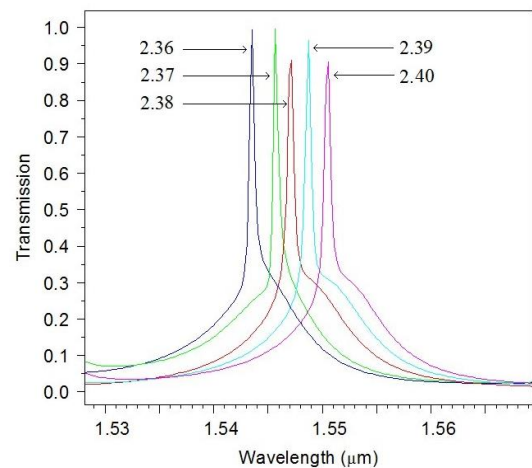


Fig. 9. The output spectra for different values of  $n_b$  and  $n_y$ .

Table 7. The output parameters of the filter as a function of  $n_b$ , and  $n_y$ .

| $n_{b,y}$ | $\Delta\lambda$ (nm) | $\lambda_{ct}$ (nm) | QF   | $P_{CE}$ (%) |
|-----------|----------------------|---------------------|------|--------------|
| 2.36      | 1                    | 1547                | 1547 | 99           |
| 2.37      | 1                    | 1549                | 1549 | 99           |
| 2.38      | 1                    | 1550                | 1550 | 91           |
| 2.39      | 1                    | 1552                | 1552 | 96           |
| 2.40      | 1                    | 1554                | 1554 | 96           |

Time response of the proposed filter is shown in Fig. 10. It demonstrates that the delay time for the filter at the output port is about 2 ps.

The results obtained from simulation demonstrate that one should do a tradeoff among output parameters respect to desired application. This makes the proposed filter as a

device with different wavelengths for optical applications.

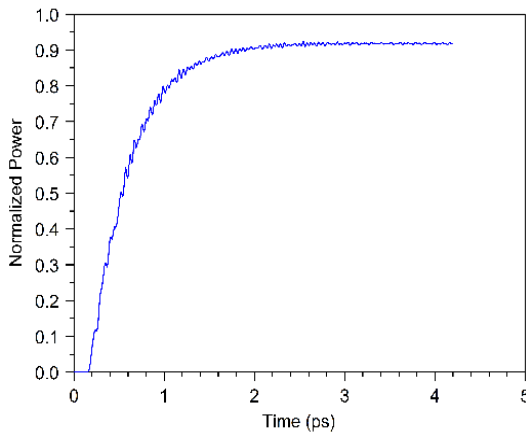


Fig. 10. Time response diagram of the proposed filter.

### III. CONCLUSION

A ring resonator based on two dimensional photonic crystal as a dropping filter is proposed to dense wavelength division multiplexing communication systems. The resonant ring consists of three different rods to simplify tuning of resonant wavelength and enhances power coupling efficiency. According to conventional Whispering Gallery Modes theory, we changed the refractive indices of rods inside the ring and propagation of light was forced to be more near the surface of the ring. Close to 99% forward dropping efficiency, quality factor as high as 1937 and pass band of 0.8 nm were obtained in the third communication window.

### REFERENCES

- [1] R. Swati and R. K. Sinha, "Design, analysis and optimization of silicon-on-insulator photonic crystal dual band wavelength demultiplexer," *Optics Commun.* vol. 282, pp. 3889-3894, 2009.
- [2] M. Gianluca, D. Paciotti, A. Marchese, M. S. Moreolo, and G. Cincotti, "2D photonic crystal cavity-based WDM multiplexer," *Photon. Nanostruc. Fund. App.*, vol. 5, pp. 164-170, 2007.
- [3] K. Sakoda, *Optical Properties of Photonic Crystals*, Springer-Verlag, Berlin, 2001.
- [4] J. D. Joannopoulos, S. G. Johnson, J. N. Winn, and R. D. Meade, *Photonic Crystals: Molding the Flow of Light*, Princeton University press, 2008.
- [5] S. Xuezheng, P. Gu, W. Shen, X. Liu, Y. Wang, and Y. Zhang, "Design and fabrication of a novel reflection filter," *App. Opt.*, vol. 46, pp. 2899-2902, 2007.
- [6] H. Alipour-Banaei and F. Mehdizadeh, "A proposal for anti-UVB filter based on one-dimensional photonic crystal structure," *Digest J. Nanomat. Biostruc.* vol. 7, pp. 367-371, 2012.
- [7] K. Mykola, X. Daxhelet, M. Gaidi, and M. Chaker, "Electronically reconfigurable superimposed waveguide long-period gratings," *J. Opt. Soc. Am. A*, vol. 19, pp. 1632-1648, 2002.
- [8] K. Ahmad and A. G. Kirk, "Composite superprism photonic crystal demultiplexer: analysis and design," *Opt. exp.*, vol. 18, pp. 20518-20528, 2010.
- [9] S. H. Kim, H. Y. Ryu, H. G. Park, G. H. Kim, Y. S. Choi, and Y. H. Lee, "Two-dimensional photonic crystal hexagonal waveguide ring laser," *Appl. Phys. Lett.* vol. 81, pp. 2499-2501, 2002.
- [10] H. Alipour-Banaei, F. Mehdizadeh, and S. Seraj mohammadi, "A novel 4-channel demultiplexer based on photonic crystal ring resonators," *Optik*, vol. 124, pp. 5964-5967, 2013.
- [11] M. A. Mansouri-Birjandi, and M. R. Rakhshani "A new design of tunable four-port wavelength demultiplexer by photonic crystal ring resonator," *Optik*, vol. 124, pp. 5923-5926, 2013.
- [12] L. Li and G. Q. Lin, "Photonic crystal ring resonator channel drop filter," *Optik*, vol. 124, pp. 2966-2968, 2013.
- [13] S. Robinson and R. Nakkeera, "Two dimensional photonic crystal ring resonator based add drop filter for CWDM systems," *Optik*, vol. 124, pp. 3430-3435, 2013.
- [14] F. Mehdizadeh, H. Alipour-Banaei, and S. Seraj mohammadi, "Channel-drop filter based on a photonic crystal ring resonator," *Optik*, vol. 125, pp. 075401-7, 2013.
- [15] R. Talebi, K. Abbasian, and A. Rostami, "Analytical modeling of quality factor for shell type microsphere resonators," *Prog. in Elec. Res. B*, vol. 30, pp. 293-311, 2011.

- [16] P. Andalib and N. Granpayeh, "Optical add/drop filter based on dual curved photonic crystal resonator," IEEE Conf. on Photonics, Germany, pp. 249–250, 2008.
- [17] F.-L. Hsiao and C. Lee, "A nano ring resonator based on 2D hexagonal lattice photonic crystals," IEEE Conf. on Optical MEMS and Nanophotonics, Florida, vol. 29, pp. 107–108, 2009.
- [18] B. Jibo, "Characteristics of 45° photonic crystal ring resonators based on square lattice silicon rods," Optoelectron. Lett. vol. 6, pp. 203–206, 2010.
- [19] M. Zetao and K. Ogusu, "Channel drop filters using photonic crystal Fabry–Perot resonators," Opt Commun., vol. 284, pp. 1192–1196, 2011.
- [20] M. Youcef, "Optical channel drop filters based on photonic crystal ring resonators," Opt. Comm. vol. 285, pp. 368–372, 2012.
- [21] S. Rezaee, M. Zavvari, and H. Alipour-Banaei, "A novel optical filter based on H-shape photonic crystal ring resonators," Optik, vol. 126, pp. 2535–2538, 2015.
- [22] Y. Wang, D. Chen, G. Zhang, J. Wang, and S. Tao, "A super narrow band filter based on silicon 2D photonic crystal resonator and reflectors," Opt. Commun. vol. 363, pp. 13–20, 2016.
- [23] A. Tavousi, M. A. Mansouri-Birjandi, and M. Saffari, "Add-Drop and channel-drop optical filters based on photonic crystal ring resonators," Int. J. Commun. and Inform. Technol. vol. 1, pp. 19-24, 2012.
- [24] A. Abbaspour, H. Alipour Banaei, and A. Andalib, "The new method for optical channel drop filter with high quality factor based on triangular photonic crystal design," J. Artif. Intell. Elec. Eng. vol. 2, pp. 73-78, 2013.



**Aghil Shaverdi** was born in Ahvaz, Iran in 1988 and received the M.S. degree in electrical

engineering from Shahid Chamran University of Ahvaz, Iran in 2016. Currently, he is a researcher in photonic laboratory at Shahid Chamran University of Ahvaz and his fields of interest are photonic crystals, ring resonators, and optical integrated circuits.



**Mohammad Soroosh** received the B.Eng. degree from the Isfahan University of Technology at Isfahan in 2000 and M.Eng.Sc and Ph.D. degrees from Tarbiat Modares University at Tehran in 2003 and 2009, respectively, all in electronics. He joined the Iran Telecommunication Research Center, Tehran in 2003 where he was a researcher at optical communication group. Currently, he is an associate professor of electronics at Shahid Chamran University of Ahvaz. His research interests are in the physics and modeling of semiconductor, photonic and optoelectronic devices.



**Ehsan Namjoo** was born in Khorram Abad, Lorestan, Iran. He received a PhD degree in telecommunication engineering from Tabriz University and is presently an assistant professor in electronic engineering in Shahid Chamran University of Ahvaz. He has worked in electromagnetic waves simulations, photonic crystals, and information coding.

**THIS PAGE IS INTENTIONALLY LEFT BLANK.**